π-mesonic decay of the hypertriton

H. Kamada,[1,*] J. Golak,[2] K. Miyagawa,[3] H. Witała,[2] and W. Glöckle[1]

[1]*Institut für Theoretische Physik II, Ruhr Universität Bochum, D-44780 Bochum, Germany*
[2]*Institut of Physics, Jagellonian University, PL 30059 Cracow, Poland*
[3]*Department of Applied Physics, Okayama University of Science, Ridai-cho Okayama 700, Japan*

(Received 29 October 1997)

The π-mesonic decay of the hypertriton is calculated based on a hypertriton wave function and $3N$ scattering states, which are rigorous solutions of three-body Faddeev equations using realistic NN and hyperon-nucleon interactions. The total π-mesonic decay rate is found to be 101% of the free Λ decay rate, which is close to the experimental data. Together with the nonmesonic decay the total lifetime of $^3_\Lambda$H is predicted to be 2.56×10^{-10} sec which is 3% smaller than for the free Λ particle. The differential decay rate is evaluated as a function of the pion momentum. The decay into the $N + d + \pi$ channel is stronger than in the $3N + \pi$ channel in contrast to the situation for the nonmesonic decay. The ratio for the decay rate into ^{3}He $+ \pi^-$ to the decay rate into all channels including π^- is found to be 0.379, which is close to the experimental value. We visualize the decay into the dominant channel $p + d + \pi^-$ in a Dalitz plot. Finally we compare the polarization of the outgoing proton in free unpolarized Λ decay to the polarization of ^{3}He in unpolarized $^3_\Lambda$H decay and we compare the closely related asymmetry of π^- emitted parallel and antiparallel with respect to the spin direction for a polarized Λ to the corresponding asymmetry for a polarized $^3_\Lambda$H. [S0556-2813(98)01104-2]

PACS number(s): 21.80.+a, 21.45.+v, 23.40.−s, 27.10.+h

I. INTRODUCTION

The hypertriton, a bound state of a proton, a neutron, and a hyperon (Λ or Σ) is bound with respect to the $\Lambda - d$ threshold by 0.13 ± 0.05 MeV. We could reproduce that number [1] by solving the Faddeev equations with realistic NN forces and the Nijmegen hyperon-nucleon interaction [2]. The hypertriton decays weakly into mesonic and nonmesonic channels. The nonmesonic decay channels are $^3_\Lambda$H$\rightarrow d + n$ and $^3_\Lambda$H$\rightarrow p + n + n$. We investigated them recently using a realistic hypertriton wave function and realistic $3N$ continuum states and evaluating the weak-strong transition $\Lambda N \rightarrow NN$ by exchange of several mesons [3,4]. We included $\pi, \eta, K, \rho, \omega,$ and K^* meson exchanges. They all contribute significantly, but there is a strong interference, which leads to a result close to the one generated by the π exchange only. We found a total nonmesonic decay rate of 6.39×10^7 sec^{-1} [3,4], which is 1.7% of the free Λ-decay rate. These decays are neutron or proton induced and we discussed that the corresponding total rates cannot be separated experimentally. Under certain angular and energy restriction, they can be separated, however.

In the mesonic decay mode there are more channels: $^3_\Lambda$H$\rightarrow \pi^- (\pi^0) + {}^3He(^3H)$, $^3_\Lambda$H$\rightarrow \pi^- (\pi^0) + d + p(n)$, and $^3_\Lambda$H$\rightarrow \pi^- (\pi^0) + p + n + p(n)$. In contrast to heavier hypernuclei, where mesonic decays are Pauli blocked [5], here in the hypertriton they are by far the dominant ones. Experimentally [6] the lifetime of $^3_\Lambda$H ranges between $(2.20 +1.02 -0.53) \times 10^{-10}$ sec to $(2.64 +0.92 -0.54) \times 10^{-10}$ sec. Further there are experimental data on the branching ratio $R = \Gamma(^3_\Lambda$H$\rightarrow \pi^- + {}^3$He$)/\Gamma(^3_\Lambda$H$\rightarrow$ all π^- meson modes) rang-

ing between 0.30 ± 0.07 [6] and 0.39 ± 0.07 [7].

The mesonic decay rates have been calculated using phenomenological $^3_\Lambda$H and ^{3}He wave functions by Dalitz [8], Leon [9], and by Kolesnikov and Kopylov [10], who used $^3_\Lambda$H and ^{3}He wave functions found from variational calculations. More recently, again in a simple model the hypertriton and its mesonic decay have been reconsidered by Congleton [11]. In view of the feasibility to perform rigorous three-body calculations for bound and continuum states based on modern baryon-baryon forces it appeared worthwhile to evaluate again the mesonic decay channels using these modern technical tools. Also we hope that these renewed considerations based on modern forces will stimulate experiments on the $^3_\Lambda$H decay modes.

In Sec. II we present our formalism. Our results are shown in Sec. III. We summarize in Sec. IV. Free Λ-decay properties and technical details are deferred to the Appendixes.

II. FORMALISM

The six mesonic decay channels of the hypertriton are not independent from each other. According to the empirical $\Delta I = \frac{1}{2}$ rule, which can be realized by setting artificially the Λ state to be $|tt_z\rangle = |\frac{1}{2} \frac{-1}{2}\rangle$ in isospin and introducing $\vec{\tau}$ at the vertex for $\Lambda \rightarrow N + \pi$ the following ratios for decay rates result [5]:

$$\frac{\Gamma(^3_\Lambda H \rightarrow \pi^- + {}^3He)}{\Gamma(^3_\Lambda H \rightarrow \pi^0 + {}^3H)} = \frac{\Gamma(^3_\Lambda H \rightarrow \pi^- + p + d)}{\Gamma(^3_\Lambda H \rightarrow \pi^0 + n + d)}$$

$$= \frac{\Gamma(^3_\Lambda H \rightarrow \pi^- + p + p + n)}{\Gamma(^3_\Lambda H \rightarrow \pi^0 + n + n + p)} = 2. \quad (1)$$

Therefore we restrict ourselves to the π^- channels and introduce the following notations:

---

*Present address: Institut für Kernphysik, Fachbereich 5 der Technischen Hochschule Darmstadt, D-64289 Darmstadt, Germany.

$$\Gamma^{\text{He}} \equiv \Gamma(^3_\Lambda\text{H} \to \pi^- + {}^3\text{He}),$$

$$\Gamma^{p+d} \equiv \Gamma(^3_\Lambda\text{H} \to \pi^- + p + d),$$

$$\Gamma^{p+p+n} \equiv \Gamma(^3_\Lambda\text{H} \to \pi^- + p + p + n). \tag{2}$$

Then together with (1) we get the full mesonic decay rate:

$$\Gamma = \frac{3}{2}(\Gamma^{\text{He}} + \Gamma^{p+d} + \Gamma^{p+p+n}). \tag{3}$$

In the total momentum zero frame the three differential individual decay rates are

$$d\Gamma^{\text{He}} = \frac{1}{2}\sum_{mm_{\text{He}}} |\sqrt{3}\langle\Psi^{(-)}_{\vec{k}_\pi\vec{k}_{\text{He}}m_{\text{He}}}|\hat{O}|\Psi_{^3_\Lambda\text{H}\,m}\rangle|^2$$

$$\times \frac{d\vec{k}_\pi}{8\pi^2\omega_\pi}d\vec{k}_{\text{He}}\delta(\vec{k}_\pi+\vec{k}_{\text{He}})$$

$$\times \delta\left(M_{^3_\Lambda\text{H}} - M_{^3\text{He}} - \omega_\pi - \frac{\vec{k}^2_{\text{He}}}{6M_N}\right), \tag{4}$$

$$d\Gamma^{p+d} = \frac{1}{2}\sum_{mm_pm_d} |\sqrt{3}\langle\Psi^{(-)}_{\vec{k}_\pi\vec{k}_p\vec{k}_dm_pm_d}|\hat{O}|\Psi_{^3_\Lambda\text{H}\,m}\rangle|^2$$

$$\times \frac{d\vec{k}_\pi}{8\pi^2\omega_\pi}d\vec{k}_pd\vec{k}_d\delta(\vec{k}_\pi+\vec{k}_p+\vec{k}_d)$$

$$\times \delta\left(M_{^3_\Lambda\text{H}} - M_p - M_d - \omega_\pi - \frac{\vec{k}^2_p}{2M_N} - \frac{\vec{k}^2_d}{4M_N}\right), \tag{5}$$

and

$$d\Gamma^{p+p+n} = \frac{1}{2}\sum_{mm_1m_2m_3} |\sqrt{3}\langle\Psi^{(-)}_{\vec{k}_\pi\vec{k}_1\vec{k}_2\vec{k}_3m_1m_2m_3}|\hat{O}|\Psi_{^3_\Lambda\text{H}\,m}\rangle|^2$$

$$\times \frac{d\vec{k}_\pi}{8\pi^2\omega_\pi}d\vec{k}_1d\vec{k}_2d\vec{k}_3\delta(\vec{k}_\pi+\vec{k}_1+\vec{k}_2+\vec{k}_3)$$

$$\times \delta\left(M_{^3_\Lambda\text{H}} - 3M_N - \omega_\pi - \frac{\vec{k}^2_1}{2M_N} - \frac{\vec{k}^2_2}{2M_N} - \frac{\vec{k}^2_3}{2M_N}\right). \tag{6}$$

Here $\Psi^{(-)}$ are appropriate pion–three-nucleon scattering states, $\hat{O}$ the vertex operator ($\Lambda \to \pi^- + p$), $\Psi_{^3_\Lambda\text{H}}$ the hypertriton wave function, and $\omega_\pi = \sqrt{m^2_\pi + \vec{k}^2_\pi}$. The scattering states $\Psi^{(-)}$ are normalized to δ functions with respect to the asymptotic momenta of relative motions. The factor $\sqrt{3}$ results from antisymmetrization [12] with respect to the nucleons, which are treated as identical in the isospin formalism. Except for the choice of the relativistic energy ω_π of the pion our calculation is nonrelativistic. The binding energies ϵ are defined as usual in terms of the nucleon (M_N) and Λ mass (M_Λ):

$$M_{^3\text{He}} = 3M_N + \epsilon_{^3\text{He}},$$

$$M_{^3_\Lambda\text{H}} = 2M_N + M_\Lambda + \epsilon_{^3_\Lambda\text{H}},$$

$$M_d = 2M_N + \epsilon_d. \tag{7}$$

The individual momenta in (6) are connected to Jacobi momenta as

$$\vec{p} = \tfrac{1}{2}(\vec{k}_1 - \vec{k}_2),$$

$$\vec{q} = \frac{2}{3}(\vec{k}_3 - \tfrac{1}{2}(\vec{k}_1 + \vec{k}_2)). \tag{8}$$

The momenta in (5) are a special case with $\vec{k}_3 = \vec{k}_p$ and $\vec{k}_1 + \vec{k}_2 = \vec{k}_d$. In (4) the Jacobi momenta for ^{3}He are like in Eq. (8), but of course referring to the internal motion of ^{3}He. For the hypertriton we use a representation based on the Jacobi momenta

$$\vec{p}' = \frac{1}{2}(\vec{k}'_1 - \vec{k}'_2),$$

$$\vec{q}' = \frac{2M_N\vec{k}'_3 - M_\Lambda(\vec{k}'_1 + \vec{k}'_2)}{2M_N + M_\Lambda}. \tag{9}$$

Equations (4)–(6) refer to the total momentum zero frame and thus the individual momenta for the hypertriton obey of course $\vec{k}'_1 + \vec{k}'_2 + \vec{k}'_3 = 0$. Further we selected particle 3 to be the Λ particle.

The phase space factors are easily evaluated. The one for π^--^{3}He decay is

$$\rho^{\text{He}} \equiv \frac{1}{8\pi^2\omega_\pi}\int d\vec{k}_\pi d\vec{k}_{^3\text{He}}\delta(\vec{k}_\pi + \vec{k}_{\text{He}})\delta$$

$$\times \left(M_{^3_\Lambda\text{H}} - M_{^3\text{He}} - \omega_\pi - \frac{\vec{k}^2_{\text{He}}}{6M_N}\right)$$

$$= \frac{1}{8\pi^2}\frac{3M_Nk_\pi}{3M_N + \omega_\pi}d\hat{k}_\pi, \tag{10}$$

where $|\vec{k}_\pi|$ is kinematically fixed as

$$k_\pi = |\vec{k}_\pi| = \frac{\sqrt{(M^2_{^3_\Lambda\text{H}} + M^2_{^3\text{He}} - m^2_\pi)^2 - 4M^2_{^3_\Lambda\text{H}}M^2_{^3\text{He}}}}{2M_{^3_\Lambda\text{H}}}. \tag{11}$$

The numerical value of $|\vec{k}_\pi|$ given by this exact relativistic expression agrees within 0.022% with the corresponding number obtained from a corresponding nonrelativistical formula. The ones for $p + d + \pi^-$ and $p + p + n + \pi^-$ decays for fixed $\vec{k}_\pi$ are similar to the ones given in [3].

The exact treatment of the final continuum states in Eqs. (4)–(6) requires the solution of a four-body problem, which is beyond our present capability. Therefore we neglect the final state interaction of the pion. For its treatment in the framework of an optical potential we refer to a recent article [13]. Under the approximation of a free pion the matrix elements in Eqs. (4)–(6) shrink to ones which refer only to
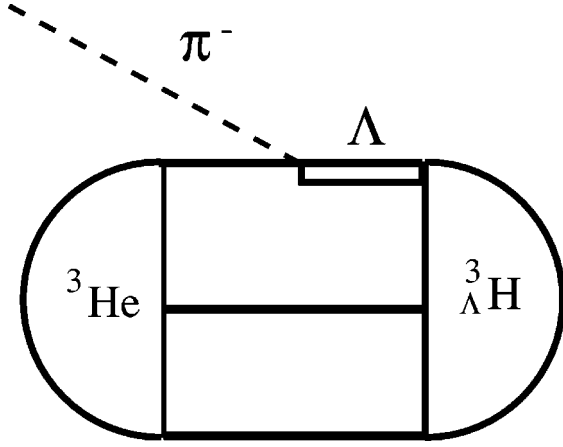
FIG. 1. The nuclear matrix element for the process $^3_\Lambda$H $\to \pi^- + ^3$He.

three baryons. The resulting operator O acting in that reduced space, related to the elementary process $\Lambda \to p + \pi^-$, is given in a relativistic notation as [5]

$$O = i\sqrt{2}\, G_F m_\pi^2 \bar{u}_N(\vec{k}_3)(A_\pi + B_\pi \gamma_5) u_\Lambda(\vec{k}_3), \qquad (12)$$

where $\bar{u}$, u are Dirac spinors and $G_F m_\pi^2 = 2.21 \times 10^{-7}$ the weak coupling constant. The constants $A_\pi = 1.05$ and $B_\pi = -7.15$ measure the parity violating and conserving parts [14,3]. The factor $\sqrt{2}$ arises from the ''spurion'' character of Λ and from $\vec{\tau} \cdot \vec{\phi}$, where $\vec{\phi}$ is the isovector pion field. In case of the $n + \pi^0$ decay that factor is (-1). In nonrelativistic reduction the simple operator results

$$O \to i\sqrt{2}\, G_F m_\pi^2 \left(A_\pi + \frac{B_\pi}{2\bar{M}} \vec{\sigma} \cdot \vec{k}_\pi \right) \qquad (13)$$

with $\bar{M} \approx (M_N + M_\Lambda)/2$. The free Λ-decay rate is briefly displayed in Appendix A. The use of the nonrelativistic reduction (13) introduces only a 2% shift for that decay rate. Finally using Eqs. (8),(9), the Λ rest frame condition, and our choice for the Λ to be particle 3 one has

$$\vec{k}_\pi = \frac{3}{2}(\vec{q}\,' - \vec{q}). \qquad (14)$$

Though we neglect the interaction of the pion with the three nucleons we treat the one for the three final nucleons exactly. This is depicted graphically in Figs. 1–3. The final state interaction among the three nucleons can be performed in analogy to electron scattering on ^{3}He [15]. We exemplify it for the nnp breakup process. For our notation in general we refer to [16].

The $3N$ scattering state expressed in Jacobi momenta, $\Psi^{(-)} \equiv \Psi^{(-)}_{pqm_1 m_2 m_3}$, is Faddeev decomposed

$$\Psi^{(-)} = (1+P)\psi^{(-)}, \qquad (15)$$

where P is the sum of a cyclical and anticyclical permutation of three objects and $\psi^{(-)}$ is one Faddeev component. It obeys the Faddeev equation
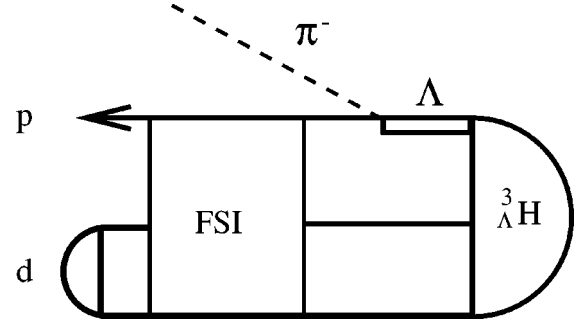

FIG. 2. The nuclear matrix element for the process $^3_\Lambda$H $\to \pi^- + p + d$.

$$\psi^{(-)} = \phi^{(-)} + G_0^{(-)} t^{(-)} P \psi^{(-)} \qquad (16)$$

with

$$\phi^{(-)} = (1 + G_0^{(-)} t^{(-)})\phi_0^a \qquad (17)$$

and

$$\phi_0^a = \frac{1}{\sqrt{3!}}(1 - P_{12})|\phi_0\rangle \equiv \frac{1}{\sqrt{6}}(1 - P_{12})|\vec{p}\rangle|\vec{q}\rangle. \qquad (18)$$

Here $G_0^{(-)}$ is the free three-nucleon propagator, $t^{(-)}$ the NN (off-shell) t matrix, and $1/\sqrt{6}$ takes care of the identity of the three nucleons. Note that P_{12} acts in the two-body subsystem described by the relative momentum $\vec{p}$. As shown in [3] the nuclear matrix element for the $3N$ breakup can be written as

$$\langle \Psi^{(-)}_{pqm_1 m_2 m_3}|O|\Psi_{^3_\Lambda H}\rangle = \langle \phi_0^a|(1+P)O|\Psi_{^3_\Lambda H}\rangle$$
$$+ \langle \phi_0^a|(1+P)|U\rangle, \qquad (19)$$

where $|U\rangle$ obeys the Faddeev equation

$$|U\rangle = tG_0(1+P)O|\Psi_{^3_\Lambda H}\rangle + tG_0 P|U\rangle. \qquad (20)$$

The action of the operator O will be described in Appendix B. The hypertriton state has a ΛNN and a ΣNN part. Though the $\Lambda - \Sigma$ conversion is crucial for the binding of the hypertriton, the ΣNN admixture is very small [1] and we neglect it. Thus we also neglect the contribution of the Σ decay, as we also did in the case of the nonmesonic decay [3].
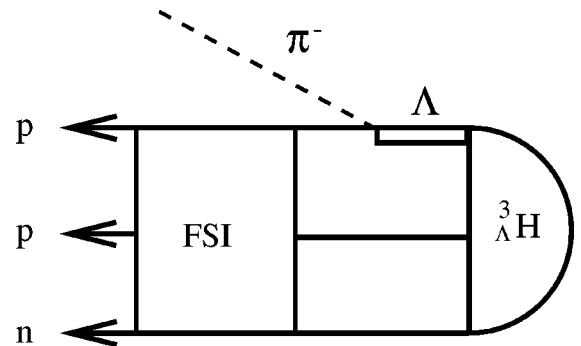

FIG. 3. The nuclear matrix element for the process $^3_\Lambda$H $\to \pi^- + p + p + n$.

TABLE I. Partial and total mesonic and nonmesonic decay rates and corresponding lifetimes.

Channel	Γ [sec^{-1}]	Γ/Γ_Λ	$\tau = \Gamma^{-1}$ [sec]
^{3}He $+\pi^-$ and ^{3}H $+\pi^0$	0.146×10^{10}	0.384	0.684×10^{-9}
$d+p+\pi^-$ and $d+n+\pi^0$	0.235×10^{10}	0.619	0.425×10^{-9}
$p+p+n+\pi^-$ and $p+n+n+\pi^0$	0.368×10^8	0.0097	0.271×10^{-7}
All mesonic channels	0.385×10^{10}	1.01	0.260×10^{-9}
$d+n$	0.67×10^7	0.0018	0.15×10^{-6}
$p+n+n$	0.57×10^8	0.015	0.18×10^{-7}
All nonmesonic channels	0.64×10^8	0.017	0.16×10^{-7}
All channels	0.391×10^{10}	1.03	2.56×10^{-10}
Expt. [6]			$2.64 +0.92 -0.54 \times 10^{-10}$
Expt. (averaged) [11]			$2.44 + 0.26 -0.22 \times 10^{-10}$

In [1] the hypertriton state has been determined in a partial wave representation and we refer to [1] for the details of our notation. Here we need only the form

$$|\Psi_{^3_\Lambda H}\rangle = \sum_\alpha \int dp\, p^2 \int dq\, q^2 |pq\alpha\rangle \Psi_\alpha(pq), \quad (21)$$

where p,q are the magnitudes of the Jacobi momenta (9) and α denotes the following set of discrete quantum numbers:

$$\alpha \equiv (ls)j\left(\lambda \frac{1}{2}\right)I(jI)J(t0)T. \quad (22)$$

Here $(ls)j$ describes the coupling of orbital angular momentum l and total spin s to the total two-body angular momentum j of the NN subsystem, $(\lambda\frac{1}{2})I$ the corresponding coupling of orbital and spin angular momentum of Λ to its total angular momentum I, $(jI)J$, the resulting jI coupling to the total angular momentum J, and finally the isospin coupling of the two-nucleon isospin $t=0$ and the isospin zero of the Λ particle to total isospin $T=0$.

Also for the evaluation of the matrix elements in (19) and the solution of the Faddeev equation (20) we work in a partial wave representation, using a complete set of basis states now for three nucleons. They are again denoted as $|pq\alpha\rangle_N$ but adding a subscript N to indicate that the Jacobi momenta are now from (8). Furthermore one has to note that this is a subset of states antisymmetrized in the subsystem of particles 1 and 2, thus $(l+s+t)$ has to be odd.

Now projecting the Faddeev equation into the basis $|pq\alpha\rangle_N$ and inserting appropriate decompositions of the unity one gets

$$\begin{aligned}
_N\langle pq\alpha|U\rangle = & \sum\!\!\!\!\!\int \sum\!\!\!\!\!\int {}_N\langle pq\alpha|tG_0(1+P)|p'q'\alpha'\rangle_{NN} \\
& \times \langle p'q'\alpha'|O|p''q''\alpha''\rangle \Psi_{\alpha''}(p''q'') \\
& + \sum\!\!\!\!\!\int {}_N\langle pq\alpha|tG_0P|p'q'\alpha'\rangle_{NN}\langle p'q'\alpha'|U\rangle.
\end{aligned}$$
$$(23)$$

This is a coupled set of integral equations, with a kernel part, which is well known [17] from $3N$ scattering, and an inhomogeneous term, whose part left of O is also familiar from electron scattering [15]. What is left as a new structure is the

application of the O matrix onto the wave function component of the hypertriton. This is given in Appendix B.

Once the amplitudes $_N\langle pq\alpha|U\rangle$ are determined, the matrix element in (19) is evaluated by quadrature in the manner described in [17] and references therein. The first matrix element in Eq. (19), the plane wave impulse approximation with respect to the nucleons, is also evaluated by the same techniques via partial wave decomposition.

III. RESULTS

We used a hypertriton wave function based on the Nijmegen 93 NN potential [18] and the Nijmegen YN interaction [2], which include the $\Lambda-\Sigma$ transitions. The number of different α quantum numbers (22), usually called channels, used in the solution of the corresponding Faddeev equation is 102. This leads to a fully converged state, which has the proper antisymmetrization among the two nucleons built in. Also the NN and YN correlations are exactly included as generated by the various baryon-baryon forces (see [1]). The ΣNN part of the state has a probability of 0.5% and will be neglected.

Let us first regard the decay channel:

$$^3_\Lambda H \rightarrow \pi^- + {}^3He.$$

In that channel we use the ^{3}He wave function generated by the Faddeev equation with the Nijmegen 93 NN interaction [18]. The kinematically fixed value of the pion momentum is $k_\pi = 117.4$ MeV/c. From (4) and (10) we obtain the total decay rate $\Gamma^{He} = 0.973 \times 10^9$ sec^{-1} as our theoretical prediction. It should be compared to the value $1.06 \pm 0.41 \times 10^9$ sec^{-1} which we estimate from the total $^3_\Lambda$H decay lifetime $\tau = (2.44 + 0.26 -0.22) \times 10^{-10}$ [11] (neglecting the nonmesonic piece), using the factor 3/2 of Eq. (3) from isospin and the ratio R (see the Introduction). The decay rates and lifetimes for both mesons are given in Table I.

Let us now ask more detailed questions in relation to that ^{3}He channel. For the free Λ decay into $p+\pi^-$ the proton turns out to be polarized as a consequence of the interference between the two operators in (13). For unpolarized Λ's the polarization of the proton in the direction of the outgoing π^- is easily evaluated as

$$P_\Lambda = \frac{\sum_{m_\Lambda} \sum_{m_p} m_p \left| \left(A_\pi + \frac{B_\pi}{2\bar{M}} \vec{\sigma}\cdot\vec{k}_\pi \right)_{m_p m_\Lambda} \right|^2}{\sum_{m_\Lambda} \sum_{m_p} \left| \left(A_\pi + \frac{B_\pi}{2\bar{M}} \vec{\sigma}\cdot\vec{k}_\pi \right)_{m_p m_\Lambda} \right|^2}$$

$$= \frac{\frac{A_\pi B_\pi}{2\bar{M}} |\vec{k}_\pi|}{A_\pi^2 + \left(\frac{B_\pi}{2\bar{M}} \right)^2 \vec{k}_\pi^2}. \tag{24}$$

P_Λ is related to the measured quantity $\alpha = -0.64 \pm 0.01$ [19] (factor 2) and agrees of course with (24), using our values for A_π and B_π. It results in $P_\Lambda = -0.322$.

Now back to the ^{3}He channel. We ask for the polarization of ^{3}He in the direction of π^- for an unpolarized $^3_\Lambda$H. It is given as

$$P_{^3\text{He}} = \frac{\sum_m \sum_{m'} m' |\sqrt{3}\langle \Psi^{(-)}_{\vec{k}_\pi \vec{k}3_{\text{He}}} m' |\hat{O}| \Psi_{^3_\Lambda \text{H}} m\rangle|^2}{\sum_m \sum_{m'} |\sqrt{3}\langle \Psi^{(-)}_{\vec{k}_\pi \vec{k}3_{\text{He}}} m' |\hat{O}| \Psi_{^3_\Lambda \text{H}} m\rangle|^2}. \tag{25}$$

We find $P_{^3\text{He}} = 0.134$, which has the opposite sign of P_Λ. This finds a simple explanation in regarding a further observable. This is the difference in the probability for π^-'s leaving in the direction of a polarized $^3_\Lambda$H to the π^- leaving opposite to that direction. This quantity can be compared to the one for the free Λ decay of a polarized Λ. In a polarized hypertriton the Λ has a small polarization $p_\Lambda = -0.166$ [1]. Therefore we expect a change of sign between the two differences and a change of the magnitude because of the nuclear wave functions. A simple calculation for the free Λ decay is

$$A^\Lambda = \frac{\left.\frac{d\Gamma^\Lambda}{d\hat{k}_\pi}\right|_{\theta_\pi=0} - \left.\frac{d\Gamma^\Lambda}{d\hat{k}_\pi}\right|_{\theta_\pi=\pi}}{\left.\frac{d\Gamma^\Lambda}{d\hat{k}_\pi}\right|_{\theta_\pi=0} + \left.\frac{d\Gamma^\Lambda}{d\hat{k}_\pi}\right|_{\theta_\pi=\pi}} = 2P_\Lambda. \tag{26}$$

Here θ_π is the angle of the emitted π^- in relation to the direction of the Λ polarization.

The corresponding quantity of the $^3_\Lambda$H decay into $\pi^- + ^3$He is

$$A^{^3_\Lambda\text{H}} = \frac{\left.\frac{d\Gamma^{\text{He}}}{d\hat{k}_\pi}\right|_{\theta_\pi=0} - \left.\frac{d\Gamma^{\text{He}}}{d\hat{k}_\pi}\right|_{\theta_\pi=\pi}}{\left.\frac{d\Gamma^{\text{He}}}{d\hat{k}_\pi}\right|_{\theta_\pi=0} + \left.\frac{d\Gamma^{\text{He}}}{d\hat{k}_\pi}\right|_{\theta_\pi=\pi}}$$

$$= \frac{\sum_{m'} |\langle \Psi^{(-)}_{\vec{k}_\pi \vec{k}3_{\text{He}}} m' |\hat{O}| \Psi_{^3_\Lambda\text{H}} m=\frac{1}{2}\rangle|^2_{\theta_\pi=0} - \sum_{m'} |\langle \Psi^{(-)}_{\vec{k}_\pi \vec{k}3_{\text{He}}} m' |\hat{O}| \Psi_{^3_\Lambda\text{H}} m=\frac{1}{2}\rangle|^2_{\theta_\pi=\pi}}{\sum_{m'} |\langle \Psi^{(-)}_{\vec{k}_\pi \vec{k}3_{\text{He}}} m' |\hat{O}| \Psi_{^3_\Lambda\text{H}} m=\frac{1}{2}\rangle|^2_{\theta_\pi=0} + \sum_{m'} |\langle \Psi^{(-)}_{\vec{k}_\pi \vec{k}3_{\text{He}}} m' |\hat{O}| \Psi_{^3_\Lambda\text{H}} m=\frac{1}{2}\rangle|^2_{\theta_\pi=\pi}}. \tag{27}$$

A detailed look into the expressions (B3) and (B4) given in Appendix B and the corresponding ones where $\hat{k}_\pi$ is opposite to the z direction reveals that

$$A^{^3_\Lambda\text{H}} = 2P_{^3\text{He}}. \tag{28}$$

Consequently also $P_{^3\text{He}}$ should be opposite in sign to P_Λ.

Let us now investigate the breakup channels:

$$^3_\Lambda\text{H} \to \pi^- + p + d \quad \text{and} \quad ^3_\Lambda\text{H} \to \pi^- + p + p + n.$$

For these channels we must solve the Faddeev equation (23). Again we use the realistic Nijmegen 93 NN interaction [18]. The technical steps are the same as in the case of the nonmesonic decay [3]. In Table I we show our theoretical predictions for the summed up rates (π^- and π^0) into the deuteron and $3N$ channels which together with the rates into the $3N$ bound states given above leads to the total rate 3.85

$\times 10^9$ sec^{-1}. It results a theoretical lifetime with respect to mesonic decay only of $\tau = 2.71 \times 10^{-10}$ sec. We see that the strongest decay goes into the $p+d$ channel followed by the transition into the three nucleon bound state ^{3}He. Both are much stronger than the decay into the $3N$ channel. For the nonmesonic decay also shown in Table I this is different. There the $n+n+p$ channel is the dominant one. Our results from [3] are reproduced for the convenience of the reader. Please note that they are larger by a factor of 3 due to an overlooked factor $\sqrt{3}$ resulting from correct antisymmetrization [4]. The total theoretical lifetime with respect to all decay channels turns out to be 2.56×10^{-10} sec which is close to the averaged value $(2.44 +0.26 -0.22) \times 10^{-10}$ sec in the range of experimental data [11]. The theoretical ratio $R = \Gamma^{\text{He}}/(\Gamma^{\text{He}} + \Gamma^{p+d} + \Gamma^{p+p+n})$ is 0.379 which is in agreement with the experimental mean value of 0.35 ± 0.04 [11].

As additional information we show in Fig. 4 the differential decay rates $d\Gamma^{p+d}/dk_\pi$ and $d\Gamma^{p+p+n}/dk_\pi$ as well as
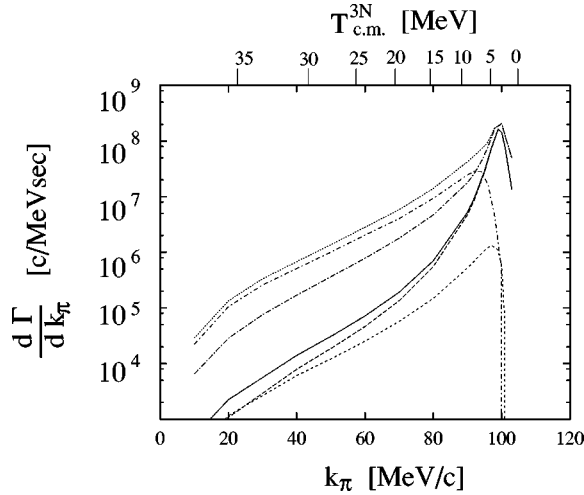
FIG. 4. Differential decay rates $d\Gamma^{p+d}/dk_\pi$ (long dashed curve), $d\Gamma^{p+p+n}/dk_\pi$ (short dashed curve), and their sum (solid curve) including FSI. Neglecting FSI the rates are drastically shifted: $d\Gamma^{p+d}/dk_\pi$ (long dashed dotted), $d\Gamma^{p+p+n}/dk_\pi$ (short dashed dotted), and their sum (dotted).

FIG. 6. A triangle chosen for the Dalitz plots in Figs. 7 and 9. The kinematically allowed events lie in the shaded area. Nearly all events occur at the right end, in the subdomain encircled by a dashed line.

their sum. These quantities result by integrating over all variables except for k_π. Both individual rates peak near the $\pi^- + p + p + n$ threshold at $k_\pi = 101.3$ MeV/c. The rate into the $p+d$ channel dominates. It is only at k_π about 20 MeV/c that the 3N channel is equally strongly populated and overtakes the $p+d$ channel for even smaller pion momenta. In Fig. 4 we also display the 3N c.m. energy $T^{3N}_{c.m.}$, which is kinematically connected to the pion momentum. At $k_\pi \approx 20$ MeV/c it reaches $T^{3N}_{c.m.} = 35$ MeV. It is around this energy where the total breakup cross section in $n+d$ scattering also overtakes the total elastic $n+d$ cross section. This is shown in Fig. 5. It is therefore tempting to interpret the outcome in Fig. 4 to result from the scattering of the nucleon arising from the weak Λ decay from the deuteron in the hypertriton. At low c.m. energies $T^{3N}_{c.m.}$ elastic scattering of that nucleon from the deuteron dominates and around $T^{3N}_{c.m.} = 35$ MeV the breakup process catches up. The stronger energy dependence in Fig. 4 in comparison to Fig. 5 is caused by the production process of the nucleon out of the Λ decay. If one switches off the final state interaction between the proton and the deuteron the decay rates are drastically shifted. Also then the

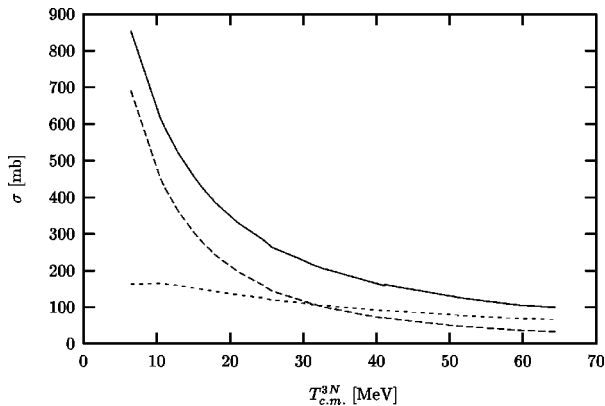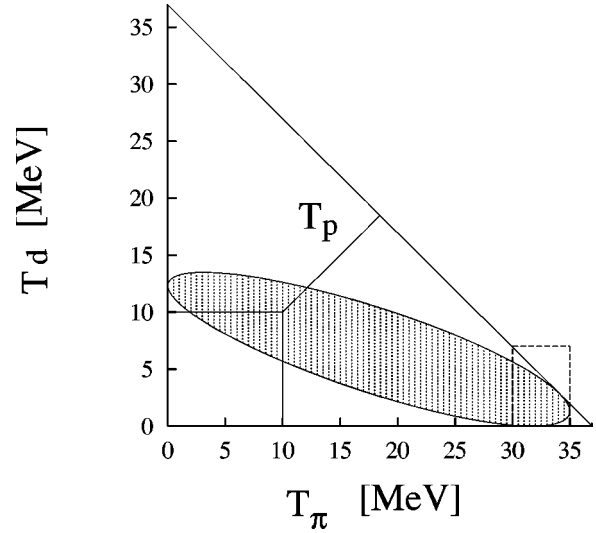three nucleon breakup dominates except near the highest pion energy.

It is conceivable that Coulomb force effects in the π^- channel, where a proton scatters off the deuteron will influence the rates. The elastic scattering in the pd channel is stronger than in the nd channel, which we calculated. We neglected the pp Coulomb force totally. This is of course a quantitative question, which should be checked in the future in a fullfledged 3N continuum calculation including the Coulomb force.

Finally we show the energy distribution of the meson, the nucleon, and the deuteron in the form of a Dalitz plot. The triangle chosen for the Dalitz plot is shown in Fig. 6. The quantity to be presented is $d\Gamma/dT_\pi dT_d$ which results from Eq. (5) by integrating over all angles. We get

$$\frac{d\Gamma}{dT_\pi dT_d} = \frac{1}{2} \sum_{mm_p m_d} \int d\phi_d d\hat{k}_\pi |\sqrt{3}\langle \Psi^{(-)}_{\vec{k}_\pi \vec{k}_p \vec{k}_d} |\hat{O}| \Psi_{^3_\Lambda H} m\rangle|^2 \frac{M_N^2}{4\pi^2},$$
(29)

where $\cos \theta_d$ is kinematically fixed. After summation over the spin magnetic quantum numbers of $^3_\Lambda$H, the proton, and the deuteron and using the momentum conserving δ function, the matrix element squared depends only on the angle θ_d between $\hat{k}_\pi$ and $\hat{k}_d$. Therefore the angular integrations in (29) are trivial and lead just to a factor $8\pi^2$.

The three kinetic energies

$$T_\pi = \sqrt{m_\pi^2 + \vec{k}_\pi^2} - m_\pi,$$

$$T_p = \frac{\vec{k}_p^2}{2M_N},$$

$$T_d = \frac{\vec{k}_d^2}{4M_N},$$
(30)

with $\vec{k}_\pi + \vec{k}_p + \vec{k}_d = 0$ sum up to the total kinetic energy $T_{c.m.} = 36.9$ MeV. As is well known the kinetic energies can
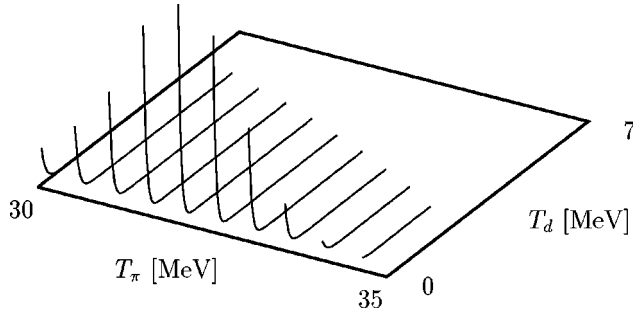

FIG. 5. Angular integrated cross sections for 3N scattering: Total nd cross section (solid curve), total elastic cross section (dashed curve), and total breakup cross section (dotted curve).

FIG. 7. The distribution $d\Gamma^{p+d}/dT_\pi dT_d$ in the subdomain of Fig. 6.

FIG. 9. The distribution $d\Gamma^{p+d}/dT_\pi dT_d$ in a subdomain of Fig. 8 for $T_d \geqslant 1$ MeV. That interference pattern results from FSI and the scale of the figure is a factor 100 smaller than in Fig. 7.

be read off as the perpendicular distances to the sides of the triangle as depicted in Fig. 6. The kinematically accessible events have to lie in the shaded area shown in Fig. 6. It turns out that essentially all events concentrate in the corner encircled by the dashed line in Fig. 6. The number of events over that subdomain is shown in Fig. 7. We see a strong rise towards the lower border of the kinematically allowed region. In other words the number of events increase with decreasing deuteron energy. For the example of $T_\pi = 32.0$ MeV we display in Fig. 8 the dependence of $d\Gamma/dT_\pi dT_d$ as a function of T_d.

Finally we display in Fig. 9 $d\Gamma/dT_\pi dT_d$ in the same subdomain as in Fig. 7 but excluding deuteron energies $T_d \leqslant 1$ MeV. The rate is down by about a factor 100 but it is more interesting, since it is generated just by final state interactions. We see a rich interference pattern.

IV. SUMMARY

The mesonic decay of the hypertriton has been calculated using a hypertriton wave function and $3N$ bound and scattering states, which are rigorous solutions of the Faddeev equations. Our results are based on the Nijmegen 93 NN potential and Nijmegen hyperon-nucleon forces, which include the Λ-Σ conversion. The standard simple particle operator for free $\Lambda \rightarrow \pi + N$ decay has been used. The interaction between the emitted π^- and the nucleons is neglected as well as Coulomb forces. We evaluated the partial decay rates into the

^{3}He $+ \pi^-$, $p + d + \pi^-$, and $p + p + n + \pi^-$ channels. The corresponding rates for π^0 emission are given by isospin symmetry (if valid). The total mesonic rate is 0.385×10^{10} sec^{-1}, which is 101% of the free Λ-decay rate. If one adds the nonmesonic decay channels that number is 103%. Thus the $^3_\Lambda$H lives a bit shorter than a free Λ.

In a previous work [3] we already discussed the nonmesonic decay channels. Thus fairly complete theoretical predictions for all decay channels of the hypertriton are available, which are based on modern forces and rigorous three-body calculations.

We also studied the momentum distribution of the emitted π^-. This distribution appears to be nicely related to nucleon-deuteron scattering initiated in the hypertriton (after decay of the Λ) as one can infer from the relation between the $p + d$ and $p + p + n$ channels.

The $p + d + \pi^-$ decay is visualized in the form of a Dalitz plot. As expected the spectrum peaks for low energetic deuterons which are present in the weakly bound hypertriton.

Finally we compared the polarization of the outgoing proton in free unpolarized Λ decay to the polarization of ^{3}He in the unpolarized hypertriton decay. They turn out to be opposite in sign, which is explained by regarding a related process. This is the difference in π^- rates for emission parallel or antiparallel to the polarized Λ and $^3_\Lambda$H respectively. The two observables, the polarization of the outgoing proton and the difference in π^- rates are equal up to a factor 2. The changes in sign result since a polarized $^3_\Lambda$H contains a polarized Λ with the spin direction pointing in the opposite direction of the polarization of the hypertriton.

Measurements of hypertriton decay properties would certainly be very useful to test these predictions based on modern dynamics.
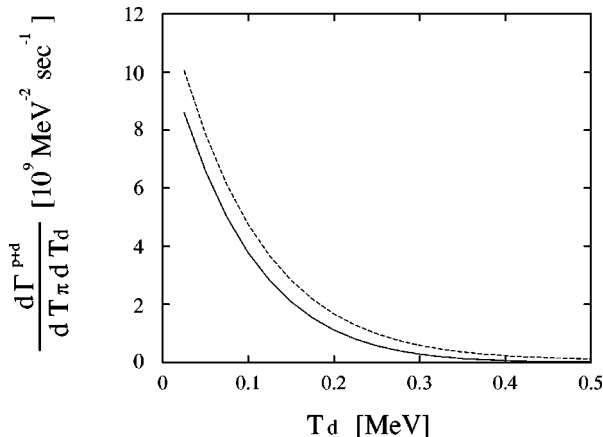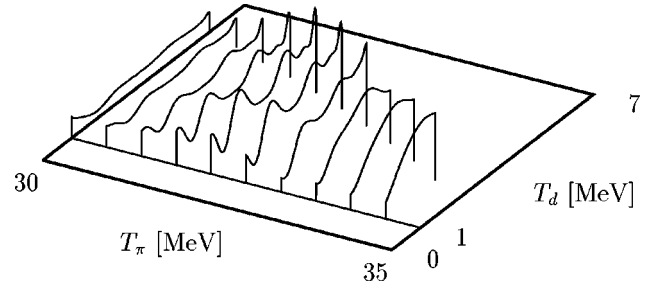
FIG. 8. The distributions $d\Gamma^{p+d}/dT_\pi dT_d$ including FSI (solid curve) and neglecting FSI (dashed curve) for fixed $T_\pi = 32$ MeV. Note that the curves for that T_π do not start at $T_d = 0$.

APPENDIX A: FREE Λ DECAY

As is well known from text books, for instance [20], the total decay rate for $\Lambda \rightarrow p + \pi^-$ and based on our notation (12) is

$$\Gamma_{\text{rel}}^{\Lambda \to p + \pi^-} = \frac{ab(f_s^2 a^2 + f_p^2 b^2)}{8\pi M_\Lambda^3}, \tag{A1}$$

with

$$a = \sqrt{(M_\Lambda + M_p)^2 - m_\pi^2},$$

$$b = \sqrt{(M_\Lambda - M_p)^2 - m_\pi^2}. \tag{A2}$$

and

$$f_s = G_F m_\pi^2 A_\pi,$$

$$f_p = G_F m_\pi^2 B_\pi. \tag{A3}$$

The momentum k_π is kinematically fixed as

$$k_\pi = |\vec{k}_\pi| = \frac{\sqrt{(M_\Lambda^2 + M_p^2 - m_\pi^2)^2 - 4 M_\Lambda^2 M_p^2}}{2 M_\Lambda}. \tag{A4}$$

The nonrelativistic calculation based on Eq. (13) yields

$$\Gamma_{\text{nonrel}}^{\Lambda \to p + \pi^-} = \frac{k_\pi}{\pi} \frac{M_p}{M_p + \omega_\pi} \left(f_s^2 + f_p^2 \frac{k_\pi^2}{4\bar{M}^2} \right). \tag{A5}$$

Both results, Eqs. (A1) and (A5) agree within 1.7%. Equations (A1) and (A5) lead to lifetimes of the Λ particle

$\frac{2}{3}[\Gamma_{\text{rel}}^{\Lambda \to p + \pi^-}]^{-1} = 2.671 \times 10^{-10}$ sec and $\frac{2}{3}[\Gamma_{\text{nonrel}}^{\Lambda \to p + \pi^-}]^{-1} = 2.717 \times 10^{-10}$ sec, respectively, which compare well to the datum $2.632 \pm 0.020 \times 10^{-10}$ sec [21].

APPENDIX B: PARTIAL WAVE REPRESENTATION OF THE OPERATOR O

We show the partial wave representation for the operator O of Eq. (13) applied onto the hypertriton state. One has

$$\langle pq\alpha m | O | \Psi_{{}^3_\Lambda H} m_{{}^3_\Lambda H} \rangle$$

$$= \sum_{\alpha'} \int dp' p'^2 \int dq' q'^2 \langle pq\alpha m | O | p' q' \alpha' \rangle$$

$$\times \langle p' q' \alpha' | \Psi_{{}^3_\Lambda H} m_{{}^3_\Lambda H} \rangle, \tag{B1}$$

where m and $m_{{}^3_\Lambda H}$ are the z components of the outgoing $3N$ state and the hypertriton, respectively. The expression can be separated into two terms:

$$\langle pq\alpha | O | \Psi_{{}^3_\Lambda H} m_{{}^3_\Lambda H} \rangle = i\sqrt{2} G_F m_\pi^2 A_\pi O_A + i\sqrt{2} G_F m_\pi^2 \frac{B_\pi}{2\bar{M}} O_B, \tag{B2}$$

with

$$O_A = \frac{1}{2} \delta_{mm_{{}^3_\Lambda H}} \sum_{\alpha'} \sqrt{\hat{j}\hat{I}\hat{I}'\hat{\lambda}'} \sqrt{\hat{\lambda}'!} (-)^j \delta_{ll'} \delta_{ss'} \delta_{jj'} \sum_{\lambda_1 + \lambda_2 = \lambda'} q^{\lambda_1} (\tfrac{2}{3} k_\pi)^{\lambda_2} \frac{1}{\sqrt{(2\lambda_1)!(2\lambda_2)!}}$$

$$\times \sum_k \hat{k}(-)^k g_{k\alpha'}(p,q,k_\pi) C(\lambda_1 k\lambda, 00) \sum_g \sqrt{\hat{g}} C(\lambda_2 kg, 00)$$

$$\times \begin{Bmatrix} g & \lambda & \lambda' \\ \frac{1}{2} & I' & I \end{Bmatrix} \begin{Bmatrix} g & I & I' \\ j & \frac{1}{2} & J \end{Bmatrix} C(Jg\tfrac{1}{2}, m0m_{{}^3_\Lambda H}) \tag{B3}$$

and

$$O_B = \frac{\sqrt{6}}{2} k_\pi \delta_{mm_{{}^3_\Lambda H}} \sum_{\alpha'} \delta_{ll'} \delta_{ss'} \delta_{jj'} (-)^{j+I'+1/2} \sqrt{\hat{j}\hat{I}\hat{I}'\hat{\lambda}\hat{\lambda}'} \sqrt{\hat{\lambda}'!} \sum_L \hat{L}(-)^L \begin{Bmatrix} \lambda' & L & 1 \\ \frac{1}{2} & \frac{1}{2} & I' \end{Bmatrix}$$

$$\times \sum_{\lambda_1 + \lambda_2 = \lambda'} q^{\lambda_1} \left(\frac{2}{3} k_\pi\right)^{\lambda_2} \frac{1}{\sqrt{(2\lambda_1)!(2\lambda_2)!}} \sum_k \sqrt{\hat{k}} g_{k\alpha'}(p,q,k_\pi) C(\lambda_1 \lambda k, 00)$$

$$\times \sum_h \sqrt{\hat{h}} C(k1h, 00) \sum_g \sqrt{\hat{g}} (-)^g C(\lambda_2 hg, 00)$$

$$\times \begin{Bmatrix} \lambda & g & L \\ I' & \frac{1}{2} & I \end{Bmatrix} \begin{Bmatrix} \lambda_1 & \lambda_2 & \lambda' \\ k & h & 1 \\ \lambda & g & L \end{Bmatrix} \begin{Bmatrix} J & I & j \\ I' & \frac{1}{2} & g \end{Bmatrix} C(Jg\tfrac{1}{2}, m0m_{{}^3_\Lambda H}), \tag{B4}$$

where

$$g_{k\alpha'}(p,q,k_\pi) = \int_{-1}^{1} dx P_k(x) \frac{\langle p, |\vec{q} + \tfrac{2}{3}\vec{k}_\pi| \alpha' | \Psi_{^3_\Lambda H} m_{^3_\Lambda H} \rangle}{|\vec{q} + \tfrac{2}{3}\vec{k}_\pi|^{\lambda'}}$$

$$(B5)$$

and where P_k is a Legendre function depending on $x = \hat{q} \cdot \hat{k}_\pi$.

We use the notation $\hat{z} = 2z + 1$. Also we assume the quantum axis to be parallel to the $\vec{k}_\pi$ direction.

The isospin part of the matrix element is not included in (B3) and (B4). It yields just the factor $\sqrt{2}$ for the π^- transition. Furthermore it leads to the requirement that the isospin of the two spectator nucleons has to be zero and that only total isospin $T = 1/2$ contributes.

[1] K. Miyagawa, H. Kamada, W. Glöckle, and V. G. J. Stoks, Phys. Rev. C **51**, 2905 (1995).

[2] P. M. M. Maessen, Th. A. Rijken, and J. J. de Swart, Phys. Rev. C **40**, 2226 (1989).

[3] J. Golak, K. Miyagawa, H. Kamada, H. Witała, W. Glöckle, A. Parreño, A. Ramos, and C. Bennhold, Phys. Rev. C **55**, 2196 (1997).

[4] J. Golak, K. Miyagawa, H. Kamada, H. Witała, W. Glöckle, A. Parreño, A. Ramos, and C. Bennhold, Phys. Rev. C **56**, 2892 (1997).

[5] J. Cohen, Prog. Part. Nucl. Phys. **25**, 139 (1990).

[6] G. Keyes *et al.*, Phys. Rev. D **1**, 66 (1970); Phys. Rev. Lett. **20**, 819 (1968); Nucl. Phys. **B67**, 269 (1973).

[7] M. Block *et al.*, in *Proceedings of the Sienna International Conference on Elementary Particles*, edited by G. Bernandini and G. P. Puppi (Societa de Fisica, Bologna, 1963), p. 62.

[8] R. H. Dalitz, Phys. Rev. **112**, 605 (1958).

[9] M. Leon, Phys. Rev. **113**, 1604 (1959).

[10] N. N. Kolesnikov and V. A. Kopylov, Sov. Phys. J. **31**, 210 (1988).

[11] J. G. Congleton, J. Phys. G **18**, 339 (1992).

[12] R. H. Dalitz and L. Liu, Phys. Rev. **116**, 1312 (1959).

[13] N. G. Kelkar, Mod. Phys. Lett. A **12**, 511 (1997).

[14] C. Bennhold, A. Ramos, D. A. Aruliah, and U. Oelfke, Phys. Rev. C **45**, 947 (1992).

[15] J. Golak, H. Kamada, H. Witała, W. Glöckle, and S. Ishikawa, Phys. Rev. C **51**, 1638 (1995).

[16] W. Glöckle, *The Quantum Mechanical Few-Body Problem* (Springer, Berlin-Tokyo, 1983).

[17] W. Glöckle, H. Witała, D. Hüber, H. Kamada, and J. Golak, Phys. Rep. **274**, 107 (1996).

[18] V. G. J. Stoks, R. A. M. Klomp, C. P. F. Terhessen, and J. J. de Swart, Phys. Rev. C **49**, 2950 (1994).

[19] R. L. Kelley *et al.*, Rev. Mod. Phys. **52**, S1 (1980); M. Roos *et al.*, Phys. Lett. **111B**, 93 (1982).

[20] K. Nishijima, *Field and Particles* (W. A. Benjamin, New York-Amsterdam, 1969).

[21] Particle Data Group, L. Montanet *et al.*, Phys. Rev. D **50**, 1173 (1994).